FORMATION OF THE NEAR-FACE STRESS FIELD UNDER THE INFLUENCE OF NATURAL AND TECHNOLOGICAL FACTORS

Krukovska V.V., Krukovskyi O.P.

M.S. Poliakov Institute of Geotechnical Mechanics of the National Academy of Sciences of Ukraine

Abstract. The mine face is a high-risk zone, where a loss of stability, an occurrence of dynamic and gas-dynamic processes, and an increase in the content of harmful gases are possible. All these negative consequences to certain extent depend on the near-face stress field. This article presents the results of numerical study of the peculiarities of its time-dependent formation in rocks with different properties, when using such means of reducing the outburst hazard as water injection and unloading cavities.

It is shown that with the course of time in the rocks around the mine working, the area of increased difference of the stress tensor components spreads, which leads to the formation of cracks of varying degrees of intensity. The maximum component of the stress tensor increases; the abutment pressure zone is formed in the near-face region. The simultaneous increase of vertical stress in the abutment pressure zone and unloading of horizontal stress leads to displacement of the coal seam in the mine working and loss of the mine face stability. If the mine working is driven through hard rocks, Q^* parameter values, as well as the maximum vertical stresses in the abutment pressure zone, are significantly increased. The zone of inelastic deformations begins to form with a long delay and has noticeably smaller dimensions. Hard rocks can withstand greater difference of the stress tensor components and greater vertical loads without breaking.

Coal moistening leads to a significant decrease in the difference of the stress tensor components in the near-face zone of the coal seam. Values of Q^* parameter in moistened coal in the three-meter near-face zone is 1.5–5 times lower than in the coal seam with a natural moisture content. The growth of the abutment pressure zone in moistened coal slows down; the zone of inelastic deformations becomes somewhat larger. The near-face stresses in the mine working with the unloading cavity is radically different from the previous cases. The peak values of Q^* parameter and maximum stress are moved to the depth of unloading cavity. At the same time, both the difference of the stress tensor components and the maximum stress remain at a low level, which corresponds to moistened coal and in a long time interval ensures deformation of the near-face zone in the elastic mode. Unloading of this zone from rock pressure occurs in two directions: in the direction of the mine face and in the direction of the unloading cavity.

Keywords: mine face, time-dependent stress field, moistening of coal seam, unloading cavity, numerical simulation.

1. Introduction

During mining, the stress field in the host rocks is formed gradually: from the moment of advancing, the host rocks begin to be unloaded from rock pressure, systems of cracks spread, the exposed surface shifts toward the mine working, delamination and destruction of the rocks occur. At the same time, the conditions for filtration processes and the occurrence of gas-dynamic phenomena change over time, which fully depends on the mode of rocks deformation.

The mine face, where collapse failure happens easily because of stress release, is a high-risk zone during the process of the mine working drivage [1, 2]. The threat of loss of the mine face stability depends on the rocks properties [3], the technologies of drivage [4, 5] and supporting [6]. In addition, there is a risk of dynamic and gas-dynamic processes occurrence, which depends on the distribution of stress values in the zones of abutment pressure and horizontal unloading [2, 7–9]. The near-face stress determines filtration permeability in this zone [10–12], and therefore, the volume and rate of gas release from gas-bearing rocks and coal, adding to the risk of increasing methane content in the mine working atmosphere.

Many factors influence the redistribution of the stress field in the mine face:
- the time passed from the advance of the mine face;
- the properties of the host rocks;

- the use of methods aimed at reducing gas release and the risk of coal and gas outbursts.

Understanding of the peculiarities of the time-dependent stress field formation in rocks with different properties and under different technological influences, is very important for reducing the above-mentioned risks and ensuring the safety of miners near the mine face. Many natural, experimental and numerical studies of the time-dependent stress field have been performed recently [13–16]. Numerical simulation of changes in stress field over time provides an opportunity to study the initial formation of the stress field around underground structures or long-term displacements of their contours. In works [17–21], the spatial and temporal evolution of the stress field in the process of tunnelling and mine working driving is studied in detail. In the calculations, the authors took into account the presence of initial stress field [18, 20] and supporting [15, 17, 20, 21], rock properties [14, 16], different rheological behaviour of soft rocks [19], and duration of outage of tunnels with different unsupported roof spans [14]. But currently, not enough attention has been paid to the peculiarities of formation of the stress field in time, which are determined by such technological factors as water injection and the creation of unloading cavities. Therefore, the aim of this study is to establish the regularities of changes in the stress field around mine working during its driving under various natural and technological influences.

2. Methods

Since most often mine workings are driven through a coal seam, and coal in the conditions of coal mines of Ukraine has a high natural gas content, the effect of gas pressure in the fracture-pore space of coal on its stress state was taken into account in the calculations. Neglecting the influence of gas pressure when calculating stress fields in gas-bearing rocks can lead to errors reaching 80% [22]. The time-dependent deformation of a gas-bearing coal-rock mass can be described by the following system of equations [23, 24]:

$$c_g \frac{\partial}{\partial t} u_i = \sigma_{ij,j} + X_i(t) + P_i(t);$$ (1)

$$Q^* = \frac{\sigma_1 - \sigma_3}{\gamma H}; \qquad P^* = \frac{\sigma_3}{\gamma H};$$ (2)

$$k_{tech} = \begin{cases} 0 & \text{if } Q^* < 0.4; \ P^* > 0.2; \\ k_{min} & \text{if } 0.4 < Q^* < 0.6; \\ 0.64Q^{*2} - 0.36Q^* + 0.02 & \text{if } 0.6 < Q^* < 1.0; \ P^* > 0.1; \\ k_{max} & \text{if } Q^* > 1.0; \ P^* < 0.1; \end{cases}$$ (3)

$$\frac{\partial p}{\partial t} = \frac{k_{tech}}{2\mu_g m} \left(\frac{\partial^2 p^2}{\partial x^2} + \frac{\partial^2 p^2}{\partial y^2} \right) + q(t),$$ (4)

where u_i – displacements, m; c_g – damping coefficient, kg/(m³·s); $\sigma_{ij,j}$ – derivatives of the stress tensor components for x and y axes respectively, Pa/m; t – time, s; $X_i(t)$ – projections of the external forces per unit volume of solid onto axes, N/m³; $P_i(t)$ – projections of forces due to gas pressure within the crack-pore space, N/m³; Q^* – geomechanical parameter characterizing difference of the stress tensor components field [22]; P^* – geomechanical parameter characterizing geostatic pressure unload of the rocks [25, 26]; σ_1, σ_3 – maximum and minimum component values of the principal stress tensor, Pa; γ – average weigh of the overlying rock seams, N/m³; H – mining depth, m; k_{tech} – filtration permeability caused by mining process, dependencies are built based on the analysis of experimental data [27-29]; $k_{\min}$ – minimum value of the permeability coefficient required for the beginning of a filtration process, m²; $k_{\max}$ – permeability value within the breaking zone, m²; p – gas pressure, Pa; μ_g – gas viscosity, Pa·s; m – rock porosity, %; q – gas release function, that simulates methane desorption.

The problems of stress research in the rocks around the mine working were solved in the elastic-plastic formulation [30, 31] using the Coulomb-Mohr strength criterion [32, 33]. The initial and boundary conditions set are:

$$\sigma_{yy}\big|_{t=0} = \gamma H; \quad \sigma_{xx}\big|_{t=0} = \lambda \gamma H; \quad u_x\big|_{t=0} = 0; \quad u_y\big|_{t=0} = 0; \quad p\big|_{t=0} = p_0; \quad (5)$$

$$u_x\big|_{\Omega_1} = 0; \quad u_y\big|_{\Omega_2} = 0; \quad p\big|_{\Omega_3} = p_{at}; \quad p\big|_{\Omega_4(t)} = p_0; \quad (6)$$

where λ – the side thrust coefficient; p_0 – formation methane pressure, Pa; Ω_1 – the vertical boundaries of the outer contour; Ω_2 – the horizontal boundaries of the outer contour; Ω_3 – the mine working contour; $\Omega_4(t)$ – the time-dependent boundary of the filtering area; p_{at} – air pressure, Pa.

The finite element method [34, 35] was used to solve equations (1)-(4) with initial and boundary conditions (5)-(6). The stress state of rocks around the mine working was analysed using parameters Q^* and P^* from equation (2) and the following:

- Lode-Nadai parameter μ_σ characterizing the type of stress state

$$\mu_\sigma = \frac{2\sigma_2 - \sigma_1 - \sigma_3}{\sigma_1 - \sigma_3};$$

- reduced maximum component of the principal stress tensor ($\sigma_1 / \gamma H$);
- reduced horizontal and vertical components of the stress tensor ($\sigma_x / \gamma H$, $\sigma_y / \gamma H$).

3. Problem definition

The paper examines the influence of various technological factors on the distribution of stresses in a 3-m-high mine face located at a depth of 1200 m. The thickness

of the coal seam is 1.5 m, the compressive strength $\sigma_c = 10.4$ MPa. The rock in the roof and floor of the coal seam is argillite, $\sigma_c = 17.3$ MPa, figure 1.
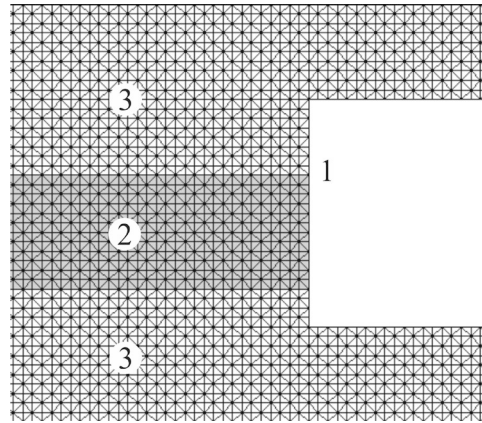
1 – mine face; 2 – coal seam; 3 – argillite

Figure 1 – The central fragment of the finite-element grid

In the calculations, it was assumed that $p_0 = 8$ MPa, $p_{at} = 0.1$ MPa, $\lambda = 1$. The duration of one time step i is approximately 2.5 hours.

4. Time change of the near-face stress under the influence of natural and technological factors

4.1 Time change of the near-face stress field

The change of the stress field was investigated starting from the moment of the face advancing. Usually, the maximum outage of a mine face is equal to the duration of a repair shift, namely 6-8 hours. But we analysed the near-face stress for 2-3 days in order to track the consequences when drivage stops. Figures 2-7 present the results of numerical calculations of the geomechanical parameters in the near-face zone.

We can see that with the course of time in the rocks around the mine working, the area of increased difference of the stress tensor components spreads (figure 2a), which leads to the formation of cracks of varying degrees of intensity. With volumetric loading in the region of beginning of microcracking ($0.4 < Q^* < 0.6$), there is an accumulation of single, non-interacting defects [36]. Beyond the limits of elasticity and upon reaching the strength limit, which corresponds to the region of intense crack formation ($0.6 < Q^* < 1.0$), uncontrollable crack growth occurs. At this stage, deformations rapidly increase due to the propagation of cracks and loosening of the rock [36]. If Q^* parameter values decrease, the host rocks, and therefore the mine working, become more stable.

Figure 3 shows graphs of changes in Q^* parameter values along the horizontal line passing through the centre of the coal seam at different time points. In 2 days ($i = 20$) from the moment of the face advancing, the zone where $Q^* > 0.4$ extends deep into the coal seam by 2.8 m. The maximum of difference of the stress tensor components is moved away from the mine face by a distance of up to 1.0 m in the first 20 hours and then practically does not move from this position.
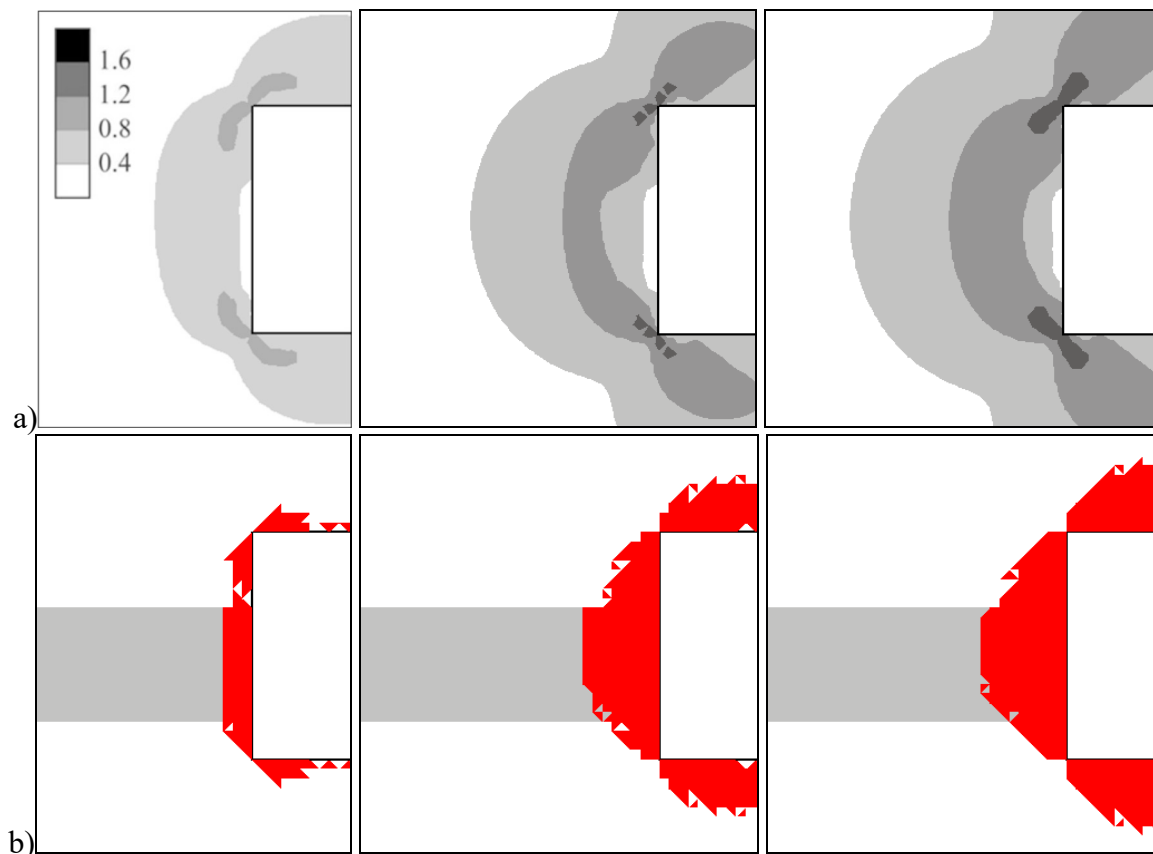
a) Q^* parameter; b) zone of inelastic deformations (red color)

Figure 2 – Distributions of stress parameters values in the moments of time:
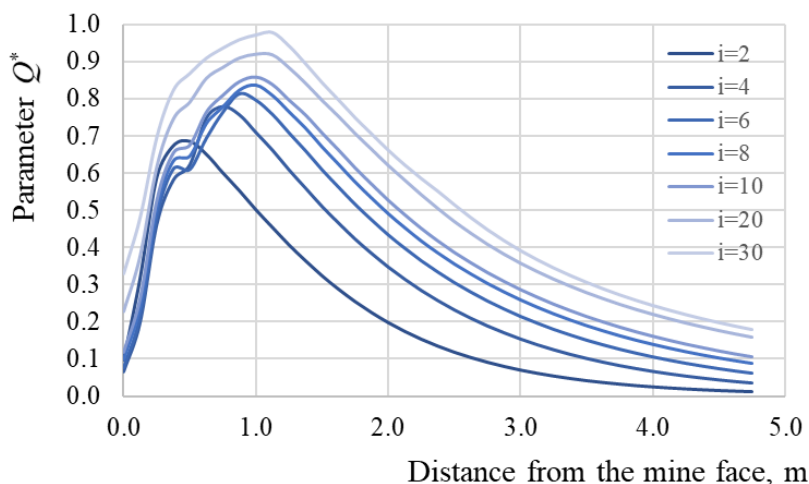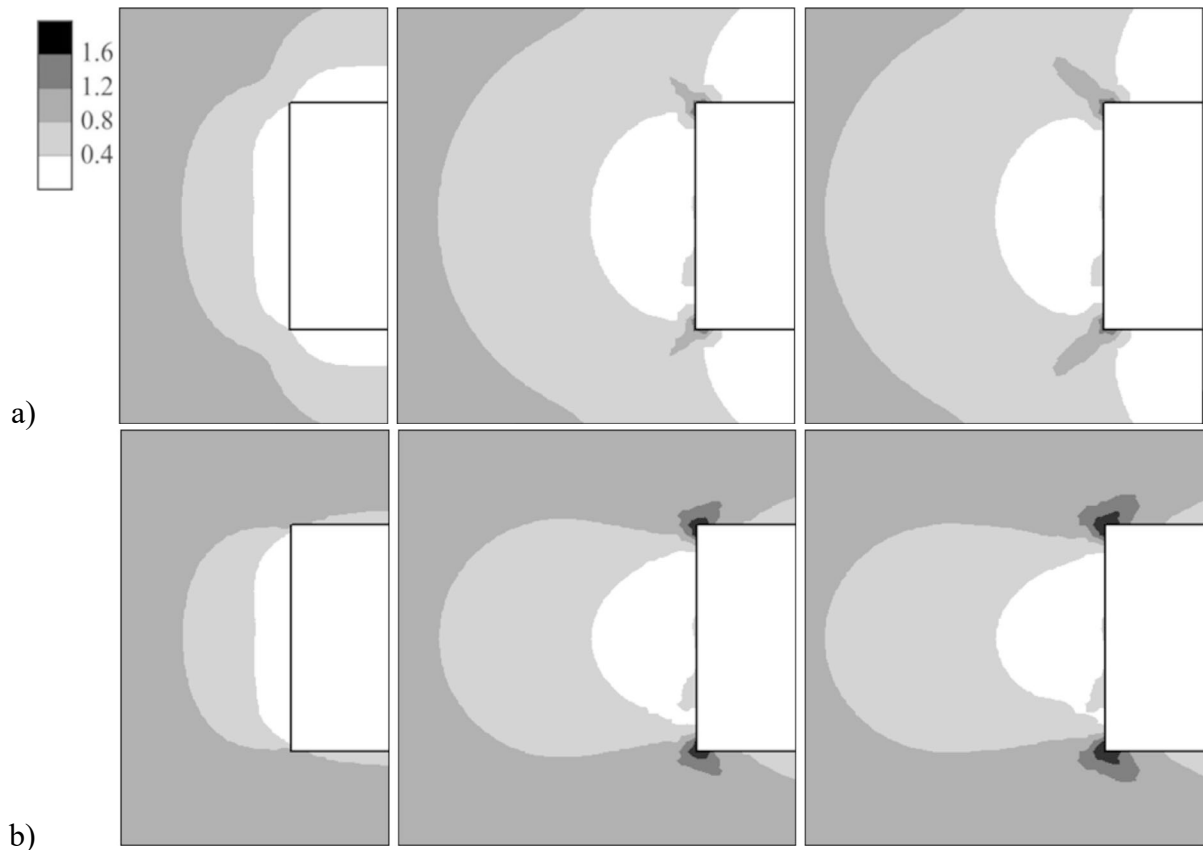$t = 5$ h, $t = 25$ h and $t = 50$ h

Figure 3 – Changes in Q^* parameter values in the coal seam

When stresses reach the strength limit of the rock, the process of macroscopic destruction begins. Brittle failure of the rock is characterized by the growth of deformations, loosening and, accordingly, the volume of the material [36]. The zone of ine-

lastic deformations, in which the strength limit was exceeded, in 2 days moves 1.1 m from the mine face deep into the coal seam, figure 2b.

a) P^* parameter; b) reduced horizontal components of the stress tensor $\sigma_x/\gamma H$

Figure 4 – Distributions of stress parameters values in the moments of time:
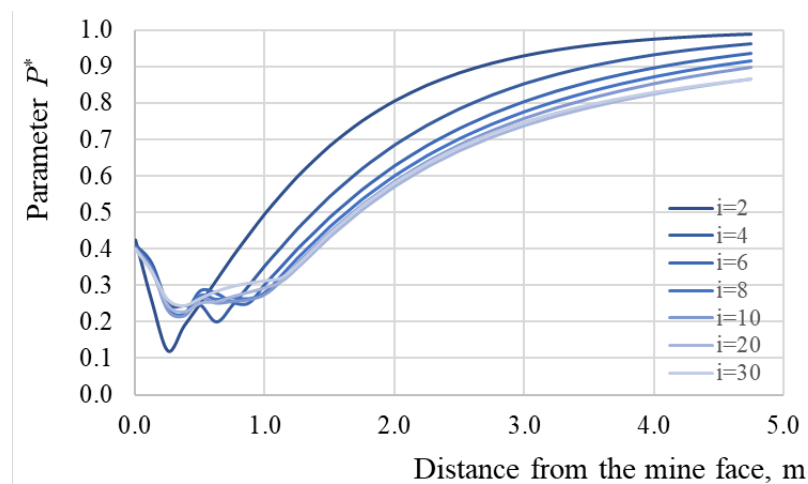$t = 5$ h, $t = 25$ h and $t = 50$ h

Figure 5 – Change of P^* parameter in the coal seam

The P^* parameter characterizes the unloading of rocks from rock pressure: if P^* parameter values approach unity, then the rocks state approaches to uniform compression

and the host rocks become more stable. In the undisturbed rock mass, at a distance from the mine working, P^* parameter values are equal to 1, in the immediate vicinity of the exposed surface they tend to zero (figures 4a and 5). Over time, the volume of un-loaded near-face rocks increases, the depth of the zone where $P^* < 0.4$ reaches 1.4 m.

It can be seen that in the coal seam, in the near-face zone, the values of the mini-mum component of the principal stress tensor and the horizontal component of the stress tensor coincide, figures 4a and 4b. Unloading of the near-face zone occurs in the horizontal direction. Therefore, in the future, we will use only the P^* parameter to ana-lyse the degree of rock unloading in this zone.

The values of the maximum component of the principal stress tensor and the verti-cal component of the stress tensor, which also coincide in the area of the coal seam, characterize abutment pressure zone, figures 6a and 6b. Over time the maximum component of the stress tensor increases (figures 6 and 7), the abutment pressure zone is formed in front of the mine face.

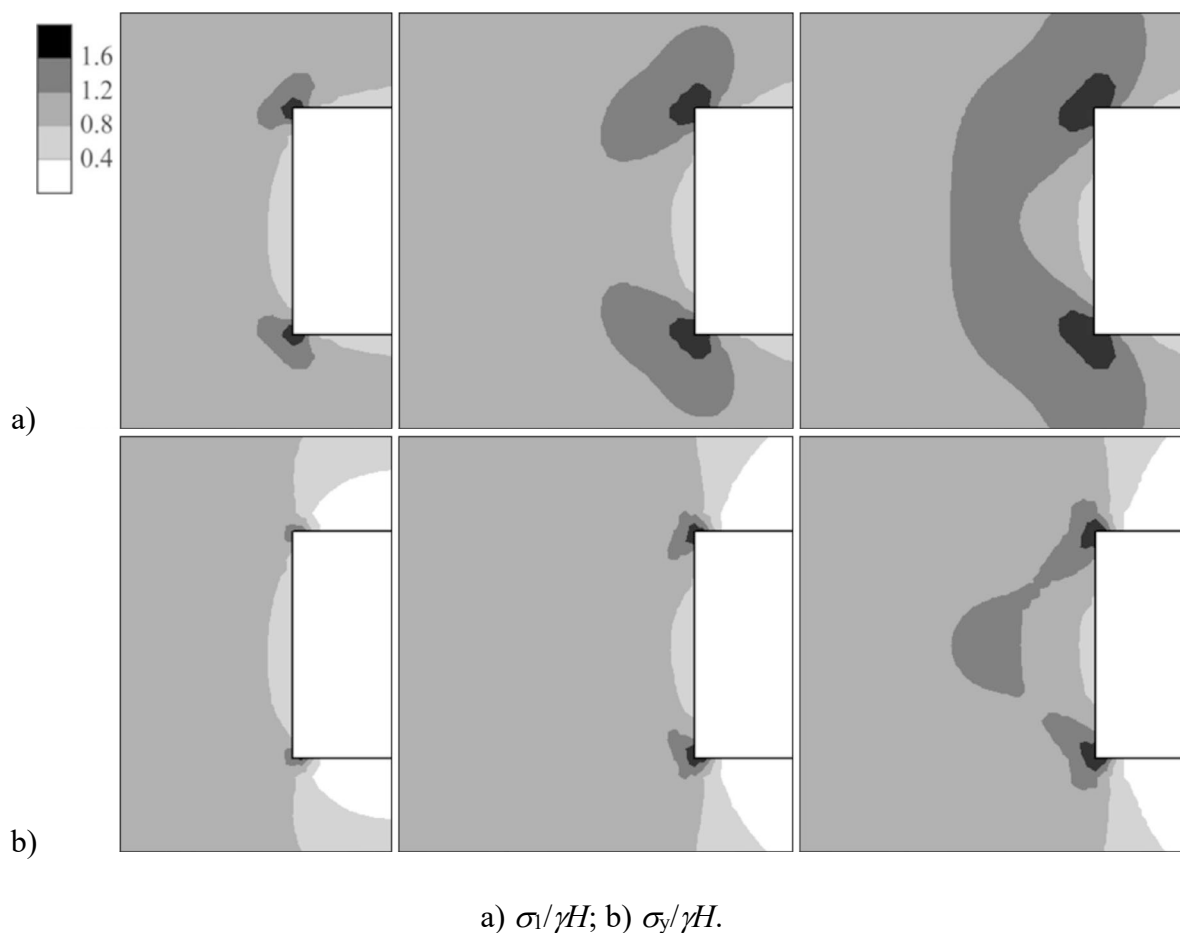a) $\sigma_1/\gamma H$; b) $\sigma_y/\gamma H$.

Figure 6 – Distributions of stress parameters values in the moments of time:
$t = 5$ h, $t = 25$ h and $t = 50$ h

An increase in the values of the reduced maximum component of the principal stress tensor by 1.3 times occurs at a distance of 1.2 m in front of the mine face. From the mark of 0.5 m and deeper into the coal seam, the maximum stresses remain high, for this zone $\sigma_1/\gamma H > 1$ (figure 7).
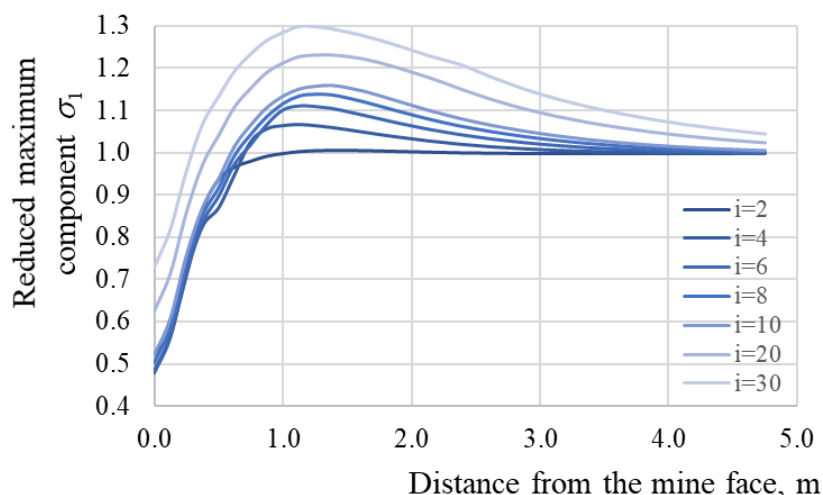
Figure 7 – Change of values of reduced maximum component of the principal stress tensor

Lode-Nadai parameter μ_σ characterizes the type of stress state; its values vary from –1 to 1. For $\mu_\sigma = 1$, the rock is in a state of generalized compression; for $\mu_\sigma = 0$ it is in a state of generalized shear; for $\mu_\sigma = -1$ it is in a state of generalized stretching. Indeed, at a sufficient distance from the mine face, where mining effects have not yet been felt, the state of the coal seam approaches uniform compression. In this zone, the parameter $\mu_\sigma \to 1$ (figure 8).
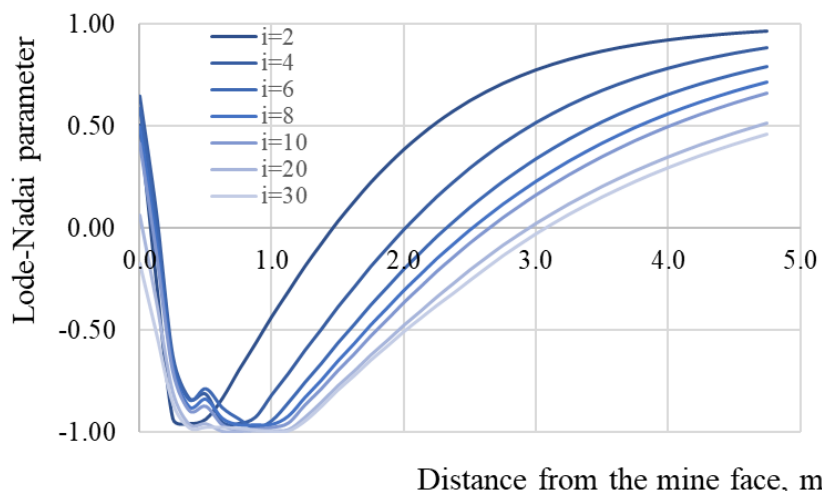

Figure 8 – Change of Lode-Nadai parameter values in the coal seam

In the near-contour area, at a distance of 0.2-1.2 m from the mine face, at different moments of time, the coal seam undergoes generalized stretching, at this interval $\mu_\sigma = -1$. Parameter P^* takes very low values here (figure 4a) and when the coal strength is low, its destruction occurs (figure 2b).

Analysing the obtained results, we see that the consequence of an outage, if for some reason the next cycle of coal and rock excavation is not performed after the end of the repair shift, there will be a significant spread of the zone of increased difference of the stress tensor components deep into the coal seam, an increase in the depth

of the zone of generalized stretching and the zone of inelastic deformations in the near-face area from 0.5 m to 1.125 m (for given initial and boundary conditions, geometric parameters and rock properties). The volume of unloaded rocks at the mine face will increase; during the time passing from the 3rd time step to the 30th time step, the depth of the zone where $P^* < 0.4$ will change from 0.8 m to 1.4 m. The maximum stresses in the abutment pressure zone will increase by 1.3 times during this time.

Thus, the redistribution of the stress field in the near-face zone of the coal seam is characterized by a simultaneous increase in the abutment pressure and unloading of the horizontal component of the stress tensor, which leads to the spread of the cracked zone deep into the coal seam, its delamination and displacement in the mine working (figure 9). This indicates a loss of the mine face stability, as well as the possibility of an active course of filtration processes in disturbed coal.
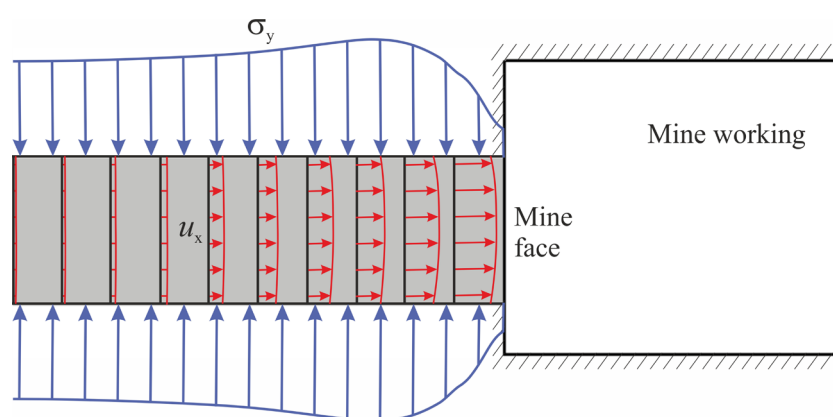

Figure 9 – The coal bed expanding in front of the mine face, $i = 10$

4.2 Effect of the rock characteristic on the stress field formation in the near-face zone

In the previous part, the near-face stresses were analysed in the case when mine working is driven through the coal seam with a rather low compressive strength. For comparison, we considered the case when mine working is driven through the hard sandstone with $\sigma_c = 34.6$ MPa. The results of the stress determination are shown in figure 10.

Comparing the obtained data with previous computations, we can note an increase in Q^* parameter values in the near-face zone. In the coal seam, the maximum difference of the stress tensor components during the studied time interval did not exceed 1.2 (figure 2a), and in the sandstone it reaches 1.6 (figure 10a). The values of the maximum vertical stresses in the abutment pressure zone are significantly higher in the case when mine working is driven through hard rocks. The region where $1.2 < \sigma_1/\gamma H < 1.6$ in figure 6a has a much smaller area than in figure 10b, on which a large region appears where $\sigma_1/\gamma H > 1.6$. At the same time, the zone of inelastic deformations in the coal seam, in contrast to the case when there is sandstone at the mine face, begins to form almost from the first hours after the face advancing (figure 2b) and during the studied time spreads deep into the seam to a depth of 1.5 times greater than in hard

sandstone (figure 10d). Hard rocks can withstand greater difference of the stress tensor components and greater vertical loads in the abutment pressure zone without breaking.
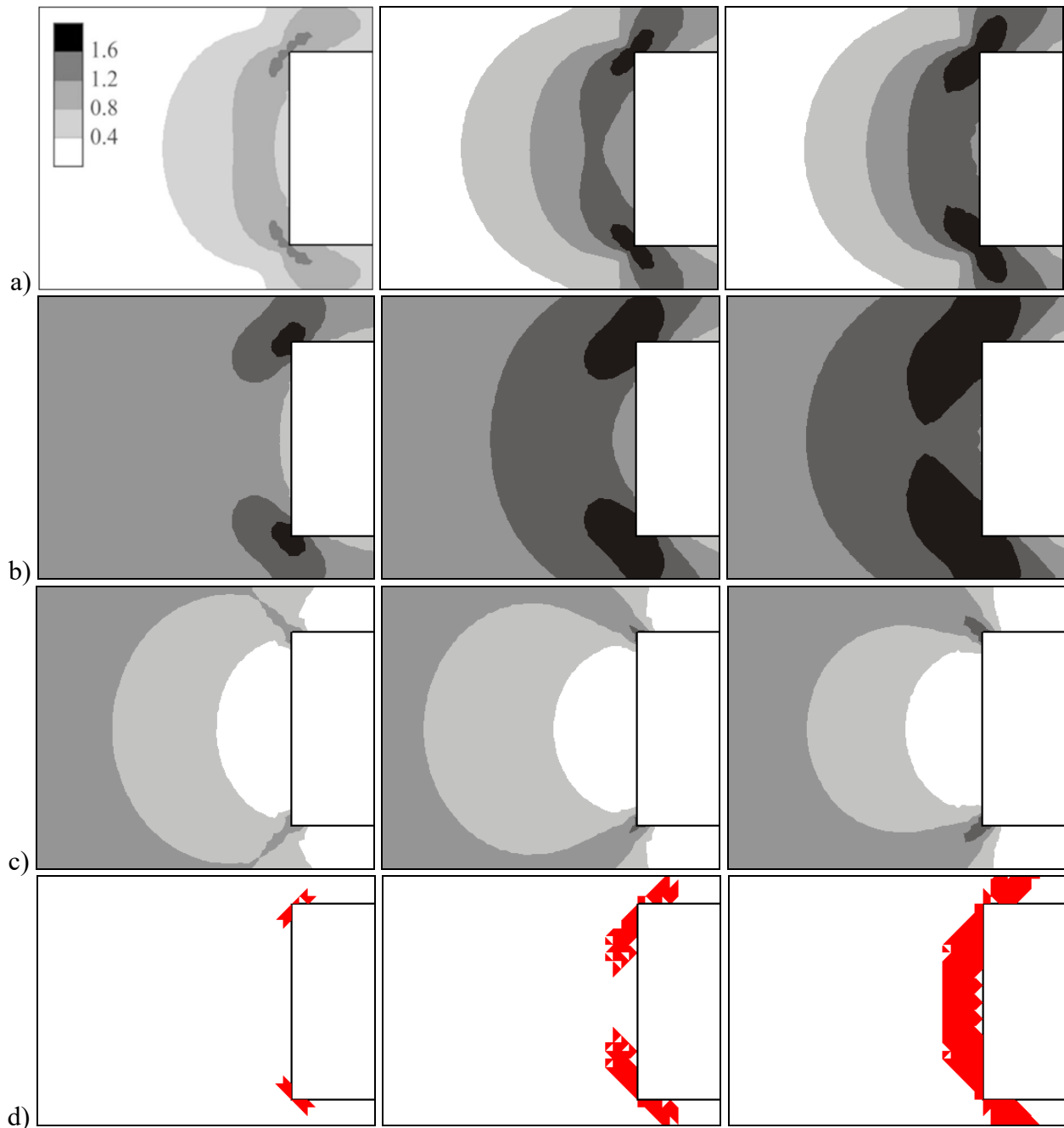
a) Q^* parameter; b) $\sigma_1/\gamma H$; c) P^* parameter; d) zones of inelastic deformations (red color).

Figure 10 – Distributions of geomechanical parameters values in the moments of time:
$t = 5$ h, $t = 25$ h and $t = 50$ h, the mine working is driven through the hard sandstone

4.3 Effect of coal moistening on the stress field formation in the near-face zone

In order to prevent instantaneous coal and gas outbursts, instantaneous coal extrusions and rock bumps, according to the standard [37], coal seam moistening and its hydraulic loosening are used. It is known that moisture saturation leads to a decrease in the strength and bearing capacity of rocks, changes the character of their behaviour af-

ter reaching the limit state [36, 38-41]. As a result of determining the modulus of elasticity E and Poisson's ratio μ of coal samples at different moisture levels, the dependences of the moisture effect on the coal deformation characteristics were established [40, 41], table. 1.

Table 1 – Moisture effect on the coal characteristics

Moisture w, %	Modulus of elasticity $E \cdot 10^{-3}$, MPa			Poisson's ratio μ		
	According to [40]	According to [41]	Average value	According to [40]	According to [41]	Average value
1	3.449	3.3	3.375	0.38	0.419	0.399
2	2.528	2.046	2.287	0.41	0.456	0.433
3	1.709	1.546	1.628	0.432	0.469	0.451
4	1.02	1.268	1.144	0.459	0.476	0.468

Tests showed that increasing the moisture content of wetting rocks can lead to a 10-fold decrease in their compressive strength [36] (figure 11).
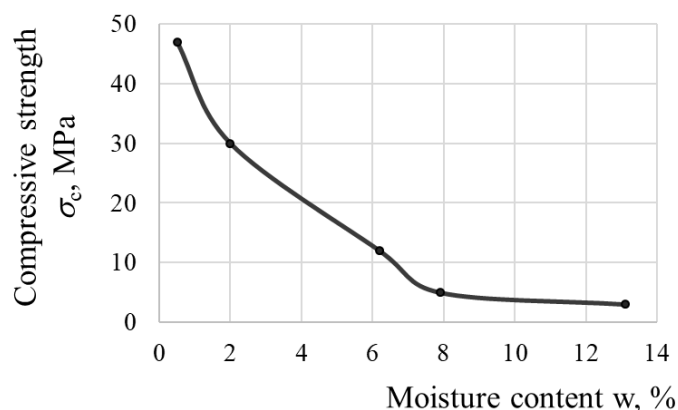

Figure 11 – Compressive strength of wetting rocks depending on their moisture content (according to [36])

Formation of the stress field was investigated in two cases: under the condition of natural moisture content $w = 1\%$ and under the condition of $w = 4\%$ after water injection into coal seam. Average data from table 1 were used in the computations, and it was assumed that the compressive strength of coal is reduced by 2 times when the moisture content reaches 4%. Figure 12 shows the results of computations of geomechanical parameters at the time step $i = 20$ ($t = 50$ h).

From figure 12a, it can be seen that water injection significantly reduces the difference of the stress tensor components in the near-face zone of the coal seam. In 10 hours after the face advancing, Q^* parameter values in moistened coal in the three-meter near-face zone is 1.5-5 times lower than in the coal seam with a natural moisture content of 1%. It is this parameter that affects the frequency and amplitude of seismoacoustic signals, which determine the position of the unloading zone by the seismoacoustic signal transmission equipment SSTE [42]. The growth of the abutment pressure zone in moistened coal slows down (figure 12b, right side). The change in coal properties leads to a decrease in the level of the maximum component

of the principal stress tensor in the near-face zone by 4-16%. At the same time, the values of the reduced minimum component of the principal stress tensor (P^* parameter) in moistened coal increase by 10-75% at various points in the coal seam (figure 12c, right side). The zone of inelastic deformations after water injection becomes somewhat larger, on the 20th time step, it increases by 11%.
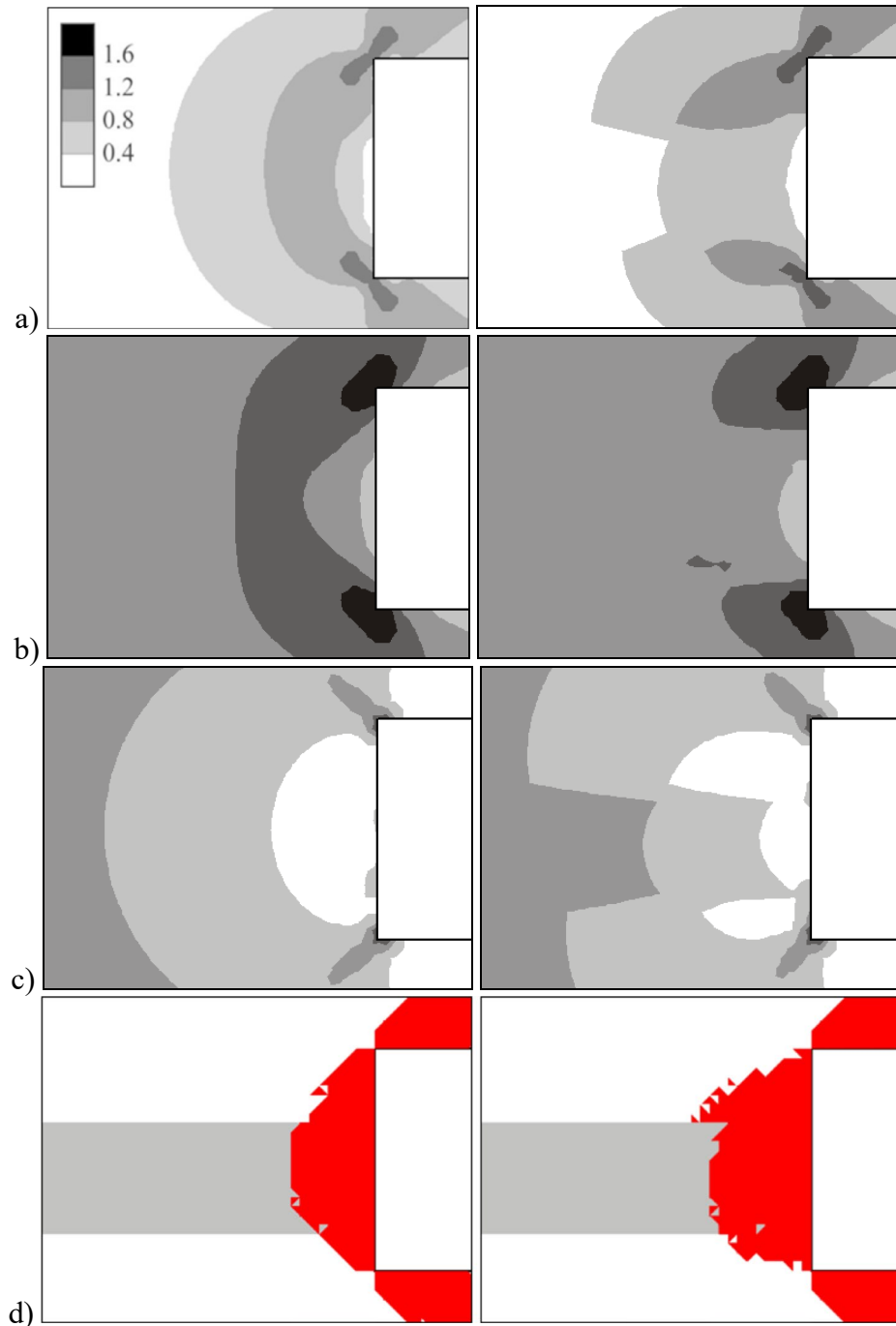
a) Q^* parameter; b) $\sigma_1/\gamma H$; c) P^* parameter; d) zones of inelastic deformations (red color).

Figure 12 – Distributions of geomechanical parameters values in the moments of time $t = 50$ h, moisture content $w = 1\%$ (left side) and $w = 4\%$ (right side)

The analysed results reflect the combined effect of two factors, namely strain relief (reduction of the modulus of elasticity) and weakening (reduction of the compressive strength) of coal during its moistening [42].

4.4 Changes in the stress field in the near-face zone when using an unloading cavity

Unloading cavities in the host rocks are formed to prevent coal and gas outbursts when mine working is driven through outburst-prone coal seams with combines or by blasting [37, 43]. In this work, it was investigated how the near-face stress field changes when using an unloading cavity 2 m deep. Figure 13 shows the results of computations of geomechanical parameters characterizing the stressed state of host rocks.

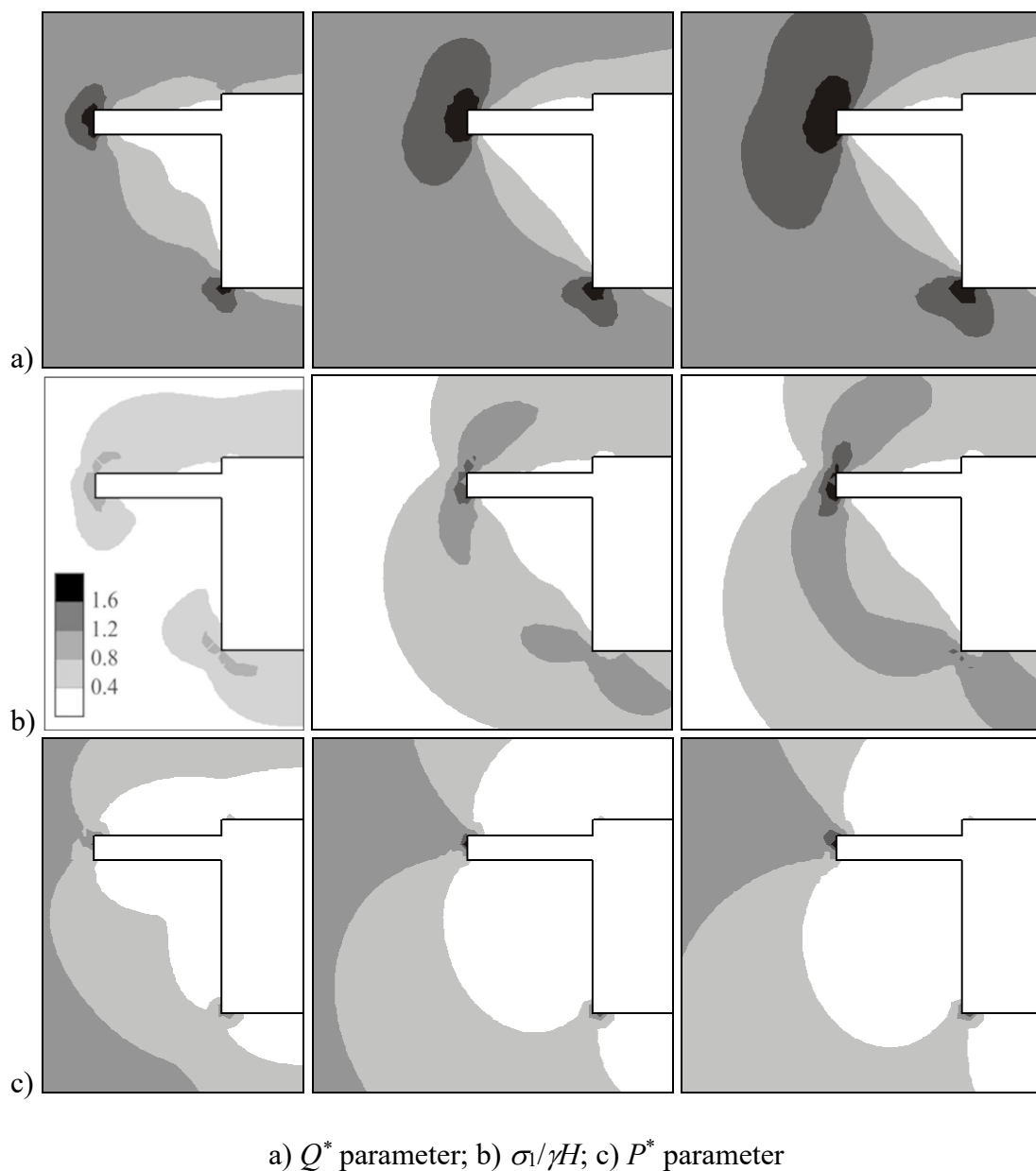a) Q^* parameter; b) $\sigma_1/\gamma H$; c) P^* parameter

Figure 13 – Distributions of geomechanical parameters values in the moments of time: $t = 5$ h, $t = 25$ h and $t = 50$ h; the mine working is driven using the unloading cavity

The distribution of the reduced maximum component of the principal stress tensor, which is shown in figure 13a, reveals a large zone located under the unloading cavity, where $\sigma_1/\gamma H < 0.4$. The length of this zone is equal to the length of the unloading cavity. In each of the cases considered above (figures 6a, 10b, 12b), the maximum stresses in the near-face zone were not lower than 0.4. On the contrary, the maximum abutment pressure was located within the two-meter near-face zone (figures 7 and 9). In the presence of the unloading cavity, the abutment pressure zone moves from the near-face region of the mine working to the near-face region of the unloading cavity (figure 13a). The spread of the zone of increased difference of the stress tensor components, in which the process of crack formation is actively occurring, deep into the coal seam slows down, and the peak of Q^* parameter values moves away from the mine face (figure 13b). The area of rocks unloaded from rock pressure, where $P^* < 0.4$, increases significantly compared to the all previous cases (figures 4a, 10c, 12c).

The zone of inelastic deformations in the coal seam until the sixth time step ($i = 6$) is practically absent, figure 14. Breaking of the near-face part of the coal seam begins from the face of unloading cavity downward and from the lower corner of the mine face upwards (figure 14c). At the time step $i = 12$, these zones are closed, covering the coal seam at a distance of 2 m from the mine face, which is equal to the depth of the unloading cavity (figure 14f). A significant part of the coal seam is separated.
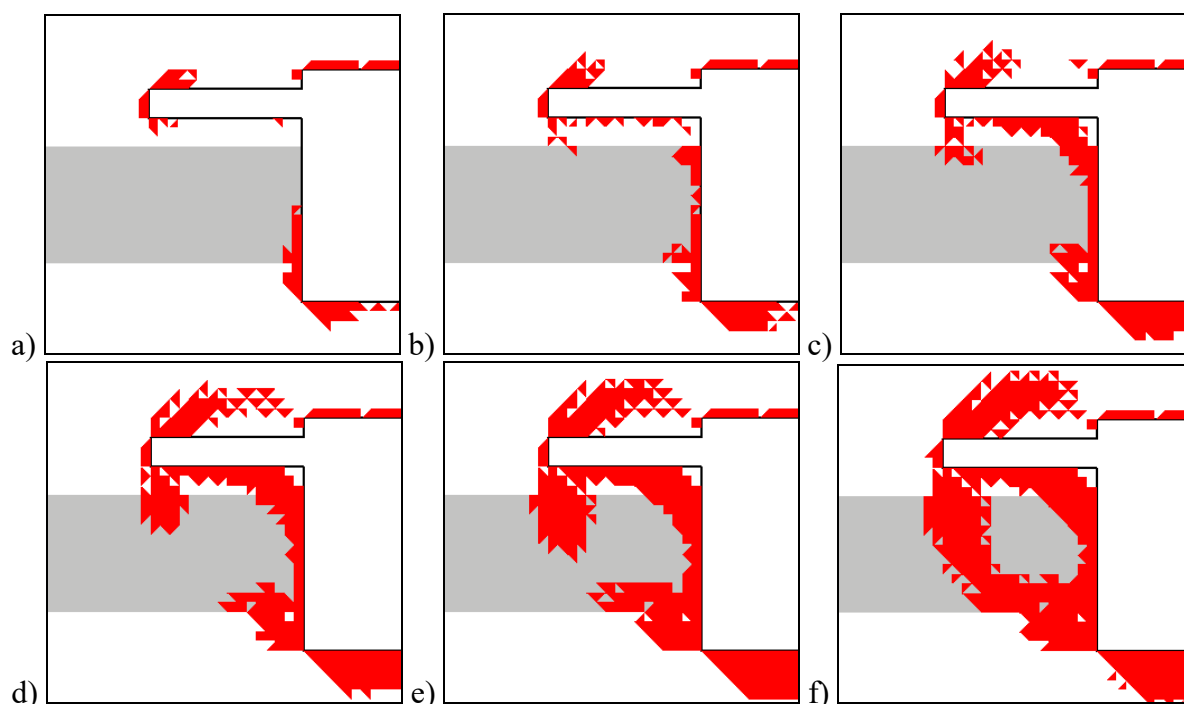

a) $i = 2$; b) $i = 4$; c) $i = 6$; d) $i = 8$; e) $i = 10$; f) $i = 12$

Figure 14 – Temporal progress of the zone of inelastic deformations (red colour) in the mine face with the unloading cavity

Thus, when using an unloading cavity, a zone completely unloaded from rock pressure is formed near the mine face, in which the occurrence of cracking and destruction processes is excluded. This zone is preserved for the first 15 hours, and then the coal seam begins to fracture slowly there. The use of an unloading cavity significantly slows down the process of fracturing, which prevents the onset of dynamic phenomena.

4.5 Comparison of near-face stress fields formed under the influence of the considered factors

In order to compare the near-face stress fields in the host rocks formed under the considered influences, the graphs of changes in geomechanical parameters were constructed along a horizontal line passing at a distance of 1.25 m from the floor of the mine working (in the centre of the coal seam, in three cases), for 4th time step, 10 hours after the face advancing, figure 15.
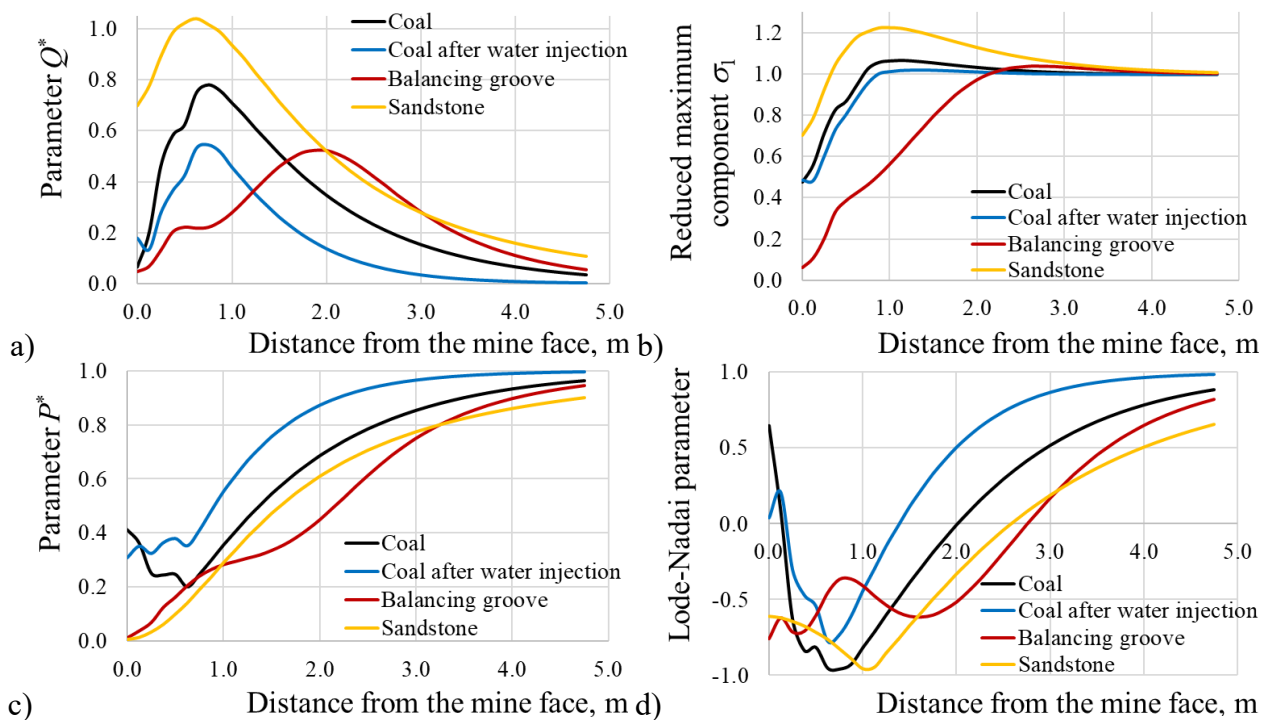
a) Q^* parameter; b) $\sigma_1/\gamma H$; c) P^* parameter; d) Lode-Nadai parameter

Figure 15 – Graphs of changes in geomechanical parameters, $i = 4$

The stress field has the maximum difference of the stress tensor components in the case when the mine working is driven through hard sandstone (figure 15a), the peak Q^* parameter value is 35% greater than in the coal seam. At a distance of 1 m from the mine face, the sandstone also withstands 15-50% higher maximum stresses (figure 15b).

Coal moistening leads to a significant decrease in the difference of the stress tensor components, at a distance of 0.75 m from the mine face where its peak is located, Q^* parameter values in the coal seam with $w = 4\%$ are 30% lower than in the seam with

$w = 1\%$. At the same time, the maximum stresses in these two cases differ little, by 3% on average. The decrease in Q^* parameter values in moistened coal occurs due to the increase in the values of the minimum component of the principal stress tensor (P^* parameter), which are the highest of all the considered cases, figure 15c. Having the lowest compressive strength, the moistened coal at the mine face is the first to enter the zone of inelastic deformations (figure 16) and begins to fracture.

The situation with the near-face stresses for the mine working with the unloading cavity is significantly different from the previous ones. The peak values of Q^* and $\sigma_1/\gamma H$ parameters are moved from a position of 0.75 m from the plane of the mine face to a distance of 2 m. At the same time, both the difference of the stress tensor components and the maximum stress remain at a low level, which corresponds to moistened coal (figures 15a and 15b) and in this time interval ensures the deformation of the near-face zone under the unloading cavity in the elastic mode (figure 16). Unloading of this zone from rock pressure occurs in two directions: in the direction of the mine face and in the direction of the unloading cavity. Therefore P^* parameter values for this case (figure 15c) is lower than the others.
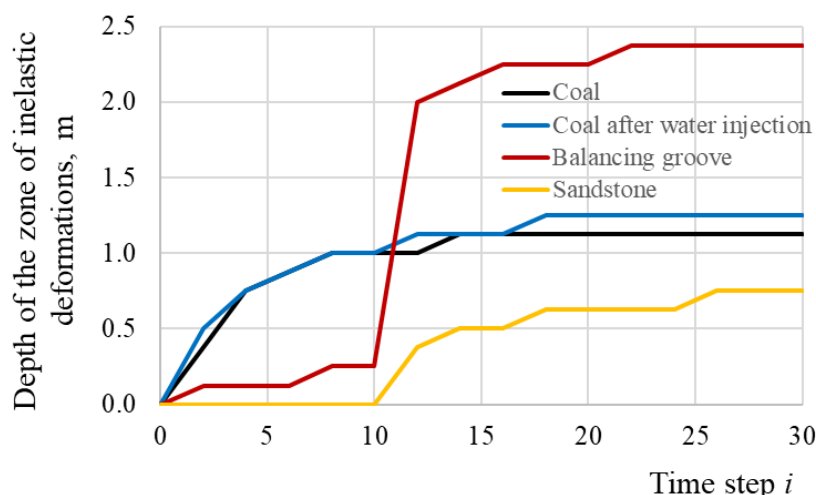

Figure 16 – Graphs of time change in the depth of the near-face zone of inelastic deformations

Lode-Nadai parameter indicates that at the time step $i = 4$, the zone of generalized stretching covers the coal seam at a distance of 0.6-1.0 m from the mine face; moistened coal seam at a distance of 0.6-0.7 m; sandstone at a distance of 0.9-1.2 m from the mine face (figure 15d). Harder sandstone withstands tensile stresses and does not undergo destruction at this time point (figure 16), unlike the coal seam. Lode-Nadai parameter values under the unloading cavity do not decrease to –1, the coal seam at a distance of up to 3.5 m from the mine face is in a stressed state close to a generalized shear.

From the graphs of the spread of the zone of inelastic deformations (figure 16), we can see that fracturing of coal with moisture content of 1% and 4% begins already from the first time iteration (2.5 hours after the mine face advance). The zones of inelastic deformations for these cases grow gradually and have approximately the same depth during the studied time interval, 1.125 and 1.25 m, respectively.

In the coal seam under the unloading cavity, the zone of inelastic deformation spreads very slowly until the time moment $i = 6$, figure 16. Fracturing of the near-face part of the coal seam occurs in a relatively short time, from 10 to 12 time steps, when the depth of the inelastic deformations zone increases from 0.25 m to 2 m (figure 16), which is equal to the depth of the unloading cavity. Further, the zone of inelastic deformations continues to increase deep into the coal seam up to 2.4 m.

The growth of the inelastic deformations zone in harder rocks begins much later, a day after the mine face advancing, and in 3 days it spreads only 0.75 m deep into the coal seam.

5. Conclusions

With the help of numerical simulation methods, the peculiarities of redistribution of the near-face stress field were investigated: time change of stress; in rocks with different properties; under various technological influences. Stresses fields, parameters for their analysis, zones of inelastic deformations were calculated for the specified cases.

It is shown that with the course of time in the rocks around the mine working, the area of increased difference of the stress tensor components spreads, which leads to the formation of cracks of varying degrees of intensity. The maximum component of the stress tensor increases by 1.3 times during the considered time; the abutment pressure zone is formed in the near-face region. In the near-contour area, at a distance of 0.2-1.2 m from the mine face, at different moments of time, the coal seam undergoes generalized stretching, at this interval Lode-Nadai parameter is equal to -1. The zone of inelastic deformations, in which the strength limit is exceeded, moves from the surface of the mine face deep into the coal seam. The simultaneous increase of the abutment pressure and unloading of the horizontal component of the stress tensor leads to spread of the cracked zone deep into the massif, displacement of the coal seam in the mine working and loss of the mine face stability. If the mine working is driven through hard rocks, the difference of the stress tensor components, as well as the maximum vertical stresses in the abutment pressure zone, are significantly increased. At the same time, the zone of inelastic deformations begins to form with a long delay and has noticeably smaller dimensions. Hard rocks can withstand greater difference of the stress tensor components and greater vertical loads without breaking.

Coal moistening leads to a significant decrease in the difference of the stress tensor components in the near-face zone of the coal seam. In 10 hours after the face advancing, Q^* parameter values in moistened coal in the three-meter near-face zone is 1.5-5 times lower than in the coal seam with a natural moisture content. The growth of the abutment pressure zone in moistened coal slows down; the zone of inelastic deformations becomes somewhat larger.

The near-face stresses in the mine working with the unloading cavity are radically different from the previous cases. The peak Q^* and $\sigma_1/\gamma H$ parameters values are moved from the position of 0.75 m from the plane of mine face to the depth of unloading cavity. At the same time, both the difference of the stress tensor components and the maximum stress remain at a low level, which corresponds to moistened coal

and, in a long time interval, ensures deformation of the near-face zone in the elastic mode. Unloading of this zone from rock pressure occurs in two directions: in the direction of the mine face and in the direction of the unloading cavity, therefore P^* parameter values for this case is lower than the others.

REFERENCES

1. Pan, Q. and Dias, D. (2016), "The effect of pore water pressure on tunnel face stability, *International Journal For Numerical And Analytical Methods In Geomechanics*", vol. 40, pp. 2123–2136. https://doi.org/10.1002/nag.2528

2. Wei, Y., Baiquan, L., Cheng, Z., Xianzhong, L., Xin, S. and Chao, Z. (2012), "A new technology for coal and gas control based on the in situ stress distribution and the roadway layout", *International Journal of Mining Science and Technology*, vol. 22, issue 2, pp.145–149. https://doi.org/10.1016/j.ijmst.2011.08.002

3. Pelli, F., Kaiser, P.K. and Morgenstern, N.R. (1995), "Effects of Rock Mass Anisotropy and Non-Linearity on the Near Face Stresses in Deep Tunnels", *Rock Mechanics and Rock Engineering*, vol. 28, no. 2, pp. 125–132. https://doi.org/10.1007/BF01020065

4. Liu, C. (2018), "Research on Deep-Buried Roadway Surrounding Rock Stability and Control Technology", *Geotechnical and Geological Engineering*, vol. 36, pp. 3871–3878. https://doi.org/10.1007/s10706-018-0578-8

5. Li, G., He, M. and Bai, Y. (2023), "The influence of the heterogeneity of rock mass for surrounding rock stability evaluation of a tunnel", *Bulletin of Engineering Geology and the Environment*, vol. 82, pp. 144. https://doi.org/10.1007/s10064-023-03145-z

6. Yoo, C. (2002), "Finite-element analysis of tunnel face reinforced by longitudinal pipes", *Computers and Geotechnics*, vol. 29, pp. 73–94. https://doi.org/10.1016/S0266-352X(01)00020-9

7. Xuea, D., Wanga, J., Zhaoa, Y. and Zhou, H. (2018), "Quantitative determination of mining-induced discontinuous stress drop in coal", *International Journal of Rock Mechanics and Mining Sciences*, vol. 111, pp. 1–11. https://doi.org/10.1016/j.ijrmms.2018.08.003

8. Smirnov, V.G. (2012), "Cracking in coal seams ahead of the working face", *Fizicheskie protsessyi gornogo proizvodstva*, no. 3, pp. 18–20.

9. Krukovskyi, O., Krukovska, V. and Zhang, W. (2020), "Outburst cavity formation in the working face driven along the outburst-prone coal seam", *II International Conference Essays of Mining Science and Practice. E3S Web of Conferences*, vol.168, pp. 00052. https://doi.org/10.1051/e3sconf/202016800052

10. Bai, M., Meng, F., Elsworth, D., Zaman, M. and Roegiers, J.-C. (1997), "Numerical modeling of stress-dependent permeability", *International Journal of Rock Mechanics and Mining Sciences*, vol. 34, no. 3–4, pp. 020. https://doi.org/10.1016/S1365-1609(97)00056-7

11. Ferfera, F.M.R., Sarda, J-P., Bouteca, M. and Vincke, O. (1997), "Experimental study of monophasic permeability changes under various stress paths", *International Journal of Rock Mechanics and Mining Sciences*, vol. 34, no. 3–4, pp. 037. https://doi.org/10.1016/S1365-1609(97)00087-7

12. Krukovska, V.V. (2022), "Numerical analysis of influence of coal seams water saturation after water injection on their outburst hazard", *Geo-Technical Mechanics*, no. 161, pp. 3–16. https://doi.org/10.15407/geotm2022.161.014

13. Arora, K., Gutierrez, M., Hedayat, A. and Cruz, E.C. (2021), "Time‑Dependent Behavior of the Tunnels in Squeezing Ground: An Experimental Study", *Rock Mechanics and Rock Engineering*, vol. 54, pp. 1755–1777. https://doi.org/10.1007/s00603-021-02370-w

14. Wang, M. and Cai, M. (2022) "Numerical Modeling of Stand‑Up Time of Tunnels Considering Time‑Dependent Deformation of Jointed Rock Masses", *Rock Mechanics and Rock Engineering*, vol. 55, pp. 4305–4328. https://doi.org/10.1007/s00603-022-02871-2

15. Barla, G., Debernardi, D. and Sterpi, D. (2012), "Time-Dependent Modeling of Tunnels in Squeezing Conditions", *International Journal of Geomechanics*, vol. 12, issue 6, pp. 697–710. http://dx.doi.org/10.1061/(ASCE)GM.1943-5622.0000163

16. Li, Lianchong, Liu, Hui-Hai, Birkholzer, J. and Vietor, T. (2014), "The use of two-part Hooke's model (TPHM) to model the mine-by test at Mont Terri Site, Switzerland", *Computers and Geotechnics*, vol. 58, pp. 28–46. http://dx.doi.org/10.1016/j.compgeo.2014.02.001

17. Neuner, M., Schreter, M., Gamnitzer, P. and Hofstetter, G. (2020), "On discrepancies between time-dependent nonlinear 3D and 2D finite element simulations of deep tunnel advance: A numerical study on the Brenner Base Tunnel", *Computers and Geotechnics*, vol. 119, pp. 103355. https://doi.org/10.1016/j.compgeo.2019.103355

18. Eberhardt, E. (2001), "Numerical modelling of three-dimension stress rotation ahead of an advancing tunnel face", *International Journal of Rock Mechanics and Mining Sciences*, vol. 38, pp. 499–518. https://doi.org/10.1016/S1365-1609(01)00017-X

19. Chu, Z., Wu, Z., Liu, B. and Liu, Q. (2019), "Coupled analytical solutions for deep-buried circular lined tunnels considering tunnel face advancement and soft rock rheology effects", *Tunnelling and Underground Space Technology*, vol. 94, pp. 103111. https://doi.org/10.1016/j.tust.2019.103111

20. Pellet, F., Roosefid, M. and Deleruyelle, F. (2009), "On the 3D numerical modelling of the time-dependent development of the damage zone around underground galleries during and after excavation", *Tunnelling and Underground Space Technology*, vol. 24, pp. 665–674. https://doi.org/10.1016/j.tust.2009.07.002

21. Monjezi, M., Rahmani, B.N., Torabi, S.R. and Singh, T.N. (2012), "Stability analysis of a shallow depth metro tunnel: a numerical approach", *Archives of Mining Sciences*, vol. 57, no. 3, pp. 535–545. https://doi.org/10.2478/v10267-012-0035-0

22. Krukovska, V.V., Krukovskyi, O.P., Kocherga, V.M. and Kostrytsia, A.O. (2022), "Solving coupled problems of geomechanics and gas filtration for mining safety ensuring", *Geo-Technical Mechanics*, no. 160, pp. 106–122. https://doi.org/10.15407/geotm2022.160.106

23. Krukovska, V.V. and Krukovskyi, D.O. (2017), "Method of calculation parameters of coupled processes of coal-rock massif deformation and methane filtration", *Geo-Technical Mechanics*, no. 133, pp. 123–135. http://dspace.nbuv.gov.ua/handle/123456789/138720

24. Krukovskyi, A.P. (2011), "Modelling changes of stress-strain state of solid edge during the distance of working face of mine workings", *Problems of computational mechanics and strength of structures*, no. 17, pp. 175–181. https://pommk.dp.ua/index.php/journal/article/view/206

25. Bulat, A.F. and Vynogradov, V.V. (2002), *Oporno-ankernoe kreplenie gornyih vyirabotok ugolnyih shaht* [Bearing-bolt supporting of mine workings in coal mines], Vilpo, Dnipropetrovsk, Ukraine.

26. Krukovskyi, O., Krukovska, V., Vynohradov, Y. and Dyomin, V. (2021), "Application of roof bolting to reduce water inflow into mine workings during the crossing of tectonic disturbances", *Second International Conference on Sustainable Futures: Environmental, Technological, Social and Economic Matters. E3S Web of Conferences*, vol. 280, pp. 01006. https://doi.org/10.1051/e3sconf/202128001006

27. Krukovska, V. (2006), "Preparation method of calculation of methane filtration parameters with the account a mode of stressedly-deformed state of coal-rock mass", Abstract of Ph.D. dissertation, Physical processes of mining production, M.S. Poljakov Institute of Geotechnical Mechanics under NAS of Ukraine, Dnipropetrovsk, Ukraine.

28. Kulinich, V.S. and Kulinich, S.V. (2000), "Influence of stress-strain state on gas recovery of methane-bearing rocks", *Geo-Technical Mechanics*, no. 17, pp. 152–156.

29. Kulinich, V.S., Perepelitsa, V.G., Kurnosov, S.A. and Ivanchishin, S.Ya. (2003), "Gas permeability of rocks in a multicomponent field of compressive stresses", *Geo-Technical Mechanics*, no. 42, pp. 18–24.

30. Hashiguchi, K. (2014), Elastoplasticity Theory, Springer. https://doi.org/10.1007/978-3-642-35849-4

31. Tan, C.H. (2016), "Difference solution of passive bolts reinforcement around a circular opening in elastoplastic rock mass", International Journal of Rock Mechanics and Mining Sciences, no. 81, pp. 28-38. https://doi.org/10.1016/j.ijrmms.2015.11.001.

32. Labuz, J.F. and Zang, A. (2012), "Mohr-Coulomb Failure Criterion", Rock Mechanics and Rock Engineering, no. 45, pp. 975-979. https://doi.org/10.1007/s00603-012-0281-7

33. Wang, H.-C., Zhao, W.-H., Sun, D.-S. and Guo, B.-B. (2012), "Mohr-Coulomb yield criterion in rock plastic mechan-ics", Chinese Journal of Geophysics, no. 55, pp. 733-741. https://doi.org/10.1002/cjg2.1767

34. Zienkiewicz, O.C., Taylor, R.L. and Zhu, J.Z. (2013), *The Finite Element Method: Its Basis and Fundamentals*, Butterworth-Heinemann.

35. de Borst, R., Crisfield, M.A., Remmers, J.J.C. and Verhoosel, C.V. (2012), *Non-linear finite element analysis of solids and structures*, John Wiley & Sons. https://doi.org/10.1002/9781118375938

36. Vinogradov, V.V. (1989), *Geomehanika upravleniya sostoyaniem massiva vblizi gornyih vyirabotok* [Geomechanics of rock mass state control near mine workings], Naukova dumka, Kyiv, USSR.

37. Ukraine Ministry of Coal Industry (2008), *10.1.00174088.011: 2005. Pravyla vedennya girnychikh robit na plastakh, skhylnykh do gazodynamichnykh yavyshch: Normatyvnyu dokument Minvuhlepromu Ukrainy. Standart* [10.1.00174088.011:2005. Rules for Conducting Mining Operations in Seams Prone to Gas-Dynamic Phenomena: Regulatory Document Coal Industry of Ukraine. Standard], Ukraine Ministry of Coal Industry, Kyiv, Ukraine.

38. Gua, H., Taoa, M., Lia, X., Momenib, A. and Caoc, W. (2019), "The effects of water content and external incident energy on coal dynamic behavior", *International Journal of Rock Mechanics and Mining Sciences*, no. 123, pp. 104088. https://doi.org/10.1016/j.ijrmms.2019.104088

39. Makieiev, S.Iu., Pylypenko, Yu.N., Ryzhov, H.A., Andrieiev, S.Iu. and Bobro, M.T. (2012), "Study of fluids influence on the deformation properties of coal and rocks under different loading conditions", *Suchasni resursoenerhozberihaiuchi tekhnolohii hirnychoho vyrobnytstva*, vol. 2, no. 10, pp. 73–82. http://www.kdu.edu.ua/GV_jurnal/GV_2_2012(10)/73.pdf

40. Petuhov, I.M., Litvin, V.A. and Kucherskiy, L.V. (1989), *Gornyie udaryi i borba s nimi na shahtah kizelovskogo basseyna* [Rock bursts and their control in the mines of the Kizel basin], Perm book publishing house, Perm, USSR.

41. Mineev, S.P., Usov, O.A., Poliakov, Yu.E., Bodnar, A.A. and Ukolova, T.M. (2020), "Effect of water saturation of coal samples with a central hole for their elasticity module under axle compression along the axis axle", *Physical and technical problems of mining production*, vol. 22, pp. 19–30. https://doi.org/10.37101/ftpgp22.01.002

42. Krukovskyi, O.P., Krukovska, V.V. and Usov, O.O. (2020), "Influence of coal seam treatment by water and antipyrogenes on formation of stress fields around mine working", *Geo-Technical Mechanics*, no. 150, pp. 116–126. https://doi.org/10.15407/geotm2020.150.116

43. Minieiev, S. and Kostritsa, A. (2021), "Issues of adjustment of normative documents on safe carrying out of workings by the tunneling combine on outburst-hazardous sandstone or near it at mines of Ukraine", *Journal of Donetsk National Technical University*, no. 1(6)–2(7), pp. 111–122. https://doi.org/10.31474/2415-7902-2021-1(6)-2(7)-111-122

About the authors

Krukovska Viktoriia Viktorivna, Doctor of Technical Sciences (D. Sc), Senior Researcher, Senior Researcher in Department of Pressure Dynamics Control in Rocks, M.S. Poliakov Institute of Geotechnical Mechanics of the National Academy of Sciences of Ukraine (IGTM of the NAS of Ukraine), Dnipro, Ukraine, vikakrukk@gmail.com

Krukovskyi Oleksandr Petrovych, Corresponding Member of NAS of Ukraine, Doctor of Technical Sciences (D. Sc), Deputy Director of the Institute, M.S. Poliakov Institute of Geotechnical Mechanics of the National Academy of Sciences of Ukraine (IGTM of the NAS of Ukraine), Dnipro, Ukraine, igtm@ukr.net

ФОРМУВАННЯ ПОЛЯ НАПРУЖЕНЬ У ВИБОЇ ГІРНИЧОЇ ВИРОБКИ ПІД ВПЛИВОМ ПРИРОДНИХ І ТЕХНОЛОГІЧНИХ ФАКТОРІВ
Круковська В.В., Круковський О.П.

Анотація. Вибій гірничої виробки є зоною високого ризику, де можливі втрата стійкості, розв'язування динамічних і газодинамічних процесів, підвищення вмісту шкідливих газів. Всі ці негативні наслідки певною мірою залежать від поля напружень в привибійній зоні. В цій статті представлено результати чисельного дослідження особливостей його формування в часі, в породах із різними властивостями, при застосуванні таких засобів зниження викидонебезпеки, як нагнітання води і розвантажувальні порожнини.

Показано, що з плином часу в породах навколо виробки поширюється область підвищеної різнокомпонентності поля напружень, що призводить до тріщиноутворення різного ступеню інтенсивності. Максимальна компонента тензора напружень зростає, у вибої виробки формується зона опорного тиску. Одночасне наростання вертикальних напружень в зоні опорного тиску і розвантаження горизонтальних призводить до зміщень пласта в виробку і втрати стійкості вибою. Якщо виробка проводиться по міцним породам, значення параметру Q^*, так як і максимальні вертикальні напруження в зоні опорного тиску значно підвищуються. Зона непружних деформацій у вибої виробки починає формуватися не одразу після посування вибою, а із тривалою затримкою, і має помітно менші розміри. Міцні породи витримують без руйнування більшу різнокомпонентність поля напружень і більші вертикальні навантаження.

Гідрообробка значно знижує різнокомпонентність поля напружень в привибійній зоні вугільного пласта. Значення параметра Q^* в зволоженому вугіллі в триметровій привибійній зоні в 1,5–5 разів менше, ніж в пласті з природною вологістю. Зростання зони опорного тиску в зволоженому вугіллі уповільнюється, зона непружних деформацій після гідрообробки стає дещо більшою. Напруження у вибої виробки з розвантажувальною порожниною кардинально відрізняються від попередніх випадків. Пікові значення параметру Q^* і максимальних напружень переміщуються на глибину розвантажувальної порожнини. При цьому і різнокомпонентність поля напружень, і максимальні напруження залишаються на низькому рівні, який відповідає зволоженому вугіллю і на тривалому часовому проміжку забезпечує деформування привибійної зони в пружному режимі. Розвантаження цієї зони від гірського тиску відбувається в двох напрямках: в напрямку площини вибою гірничої виробки і в напрямку розвантажувальної порожнини.

Ключові слова: вибій гірничої виробки, зволоження вугільного пласта, поле напружень, розвантажувальна порожнина, чисельне моделювання.